Acta Neuropathol (1989) 78:72–85

Acta Neuropathologica

Dithiobiuret neurotoxicity: an ultrastructural investigation of the lesion in preterminal axons and motor endplates in the rat lumbrical muscle

H. B. Jones

Institute of Neurology, Queen Square House, Queen Square, London WC1N 3BG, Great Britain

Summary. 2,4-Dithiobiuret was given i.p. to rats for 4 days at a daily dosage of 1 mg/kg and the development of the lesion associated with neuromuscular dysfunction studied in hindlimb lumbrical muscles. The first morphological indication of neurointoxication was the appearance in some motor endplates of masses of branching tubular smooth endoplasmic reticulum (SER) on day 2 which correlated with the initial functional disturbances. By the 3rd day, most motor endplates were distended by accumulations of dense-cored, lucent and synaptic vesicles, abnormally swollen mitochondria, intermediate filaments and branching, tubular SER. Evidence of collateral axonal sprouting was seen first at this time. On days 4 and 5, many motor endplates were markedly enlarged and showed axoplasmic organelle congestion. A significant increase in synaptic vesicle size was noted at these times in some terminals. Interposition of Schwann cell processes between the pre- and postsynaptic membranes and terminal retraction was now evident. Some intramuscular nerves showed hydropic Schwann cell cytoplasm with separation of the outermost myelin lamellae, mitochondrial swelling and adaxonal vacuoles as early as the 1st day. Proliferation and segregation of SER around central cores of neurofilaments was seen in myelinated nerve fibres and preterminals on the 3rd day. At this and later times accumulations of SER and swollen mitochondria were found at sites of axonal varicosities and at the paranodal constrictions at nodes of Ranvier. These ultrastructural data are discussed with regard to reduced terminal Ca^{2+} content (demonstrated by oxalate-pyroantimonate cytochemistry) and compared with the sequelae of botulinum intoxication.

Offprint requests to: H. B. Jones, Neuropharm Ltd, Bryngelen House, 2 Bryngwili RD, Hendy, Dyfed SA4 1XB, Wales, Great Britain

Key words: 2,4-Dithiobiuret – Thioimidodicarbonic diamide – Motor endplate – Neuromuscular junction – Ultrastructure

2,4-Dithiobiuret (thioimidodicarbonic diamide, DTB) is a thiourea derivative with moderate reducing properties which has been used commercially as a plant root growth promoter, polymer stabiliser, rodenticide and as an intermediate in the preparation of resins and thermoplastics (see Atchison et al. [6] for references). The demonstration of DTB neurotoxicity in rats initially by Astwood et al. [2] and later by Atchison and Peterson [3] placed into perspective the potential risk due to occupational exposure of industrial and agricultural workers. They showed that daily administration of DTB (1 mg/kg) to rats resulted in a delayed onset, flaccid, skeletal muscle weakness, which was unrelated to muscle impairment, was associated with hypothermia and ataxia and led to death of approximately 50% of the animals within 4–5 days. Surviving animals recover mobility within a few days of withdrawal of DTB but remain weak and listless for several weeks [25].

Intensive electrophysiological and pharmacological studies [4, 6, 7, 38, 39] have provided evidence that DTB-induced muscle weakness is characterised by a deficit in neuromuscular transmission represented by a reduction in acetylcholine quanta released from the presynaptic terminal. That is, the defect appears to be prejunctional and is not due to functional impairment or blockade of the acetylcholine receptor situated on the postjunctional (sarcolemmal) membrane [7].

The disruption of normal transmission of the action potential at the neuromuscular junction and the

negative influence that this might be expected to have on the trophic relationship between nerve and muscle led Kemplay [25] to undertake a morphological study of innervation patterns during the onset of muscle weakness and during recovery after withdrawal of DTB. Employing the zinc iodide-osmium tetroxide method of Akert and Sandri [1] marked increases in staining density of motor endplates and intra-muscular nerves were observed in lumbrical, soleus, tibialis anterior and sternocostalis muscles on the 3rd day of treatment, which were coincident with the onset of generalised muscle weakness. In the sternocostalis muscle, a retraction of the motor endplate resulted in a change in its shape from the normal terminal arborisation to a more 'clumped', rounded form. This occurred as early as the 3rd day and was associated in all muscles examined with terminal sprouting, although collateral axonal sprouting was present in the sternocostalis muscle only. These data provided by Kemplay [25] allude to compromise of the normal nerve/muscle functional relationship followed by the endplate's urgent response directed at its restoration which, when viewed in conjunction with diminished treadmill performance and loss of tetanic tension of gastrocnemius contractions in response to sciatic nerve stimulation [41], provides strong support for the hypothesis [4, 5] that DTB-induced muscle weakness results from an impairment of acetylcholine release at the neuromuscular junction.

The objectives of the present studies were twofold. Firstly, to determine the earliest ultrastructural alterations in motor nerves and endplates within the lumbrical muscles of rats treated with DTB for up to 5 days and to define more clearly the evolution of the pathological lesion so as to place it into the context of the development of the functional disturbances. Secondly, to gather information which might provide some insight into its mechanism of action.

Materials and methods

Preparation of dithiobiuret solution

DTB (Ash Stevens Inc, Detroit, USA) was dissolved in 50 µl dimethylsulphoxide and diluted with sterile isotonic saline to achieve a final DTB concentration of 1 mg/ml. Dosing solutions were prepared daily.

Animal maintenance and dosing regime

Two groups of 16 and 8 female Wistar rats (designated groups 1 and 2, respectively) weighing 150–160 g and supplied by Charles River, Sittingbourne, Kent were housed in plastic, solid-floored cages and fed rat cubes (Rat and Mouse Breeder Diet, B.P., Nutrition, Witham, Essex) and tap water ad libitum.

Animals were given DTB once daily by i.p. injection at a dosage level of 1 mg/kg for up to 5 days. Control animals were treated in the same way but received vehicle only. The animals' weight and condition, especially signs of neurological impairment were closely monitored.

Preparation of tissues

Under deep ether anaesthesia group 1 animals (for conventional ultrastructural studies) were killed at daily intervals by whole body perfusion with a solution of 4% glutaraldehyde in 0.1 M cacodylate buffer (pH 7.4) via the ascending aorta at an initial pressure of 150–160 mm Hg. Following further fixation in situ at 4°C overnight, the lumbrical muscles of the hindfeet were removed and washed thoroughly in the same buffer (3 × 15 min). The tissues were then immersed in a solution of 1% osmium tetroxide in 0.1 M cacodylate buffer (pH 7.2) for 2 h, dehydrated in an ascending ethanol series and 1,2-epoxypropane and finally infiltrated with and embedded in Agar 100/Araldite resin.

Semithin sections (1 µm thick) stained with toluidine blue were examined by light microscopy to determine gross changes and to select areas for preparation of ultrathin sections. Ultrathin sections (70–80 nm thick) were stained with a saturated solution of ethanolic uranyl acetate followed by lead citrate and examined in a JEOL, JEM 1200 EX transmission electron microscope at an accelerating voltage of 80 kV.

Calcium localisation

To determine the possible chelation of Ca^{2+} by DTB or elevated terminal Ca^{2+} content and sequestration within cellular compartments, calcium localisation was investigated using a slightly modified version of the method of Borgers et al. [8].

Accordingly, group 2 animals were killed at daily intervals under identical conditions by perfusion with a solution of 4% glutaraldehyde in 0.1 M cacodylate buffer (pH 7.4) containing (90 mM) potassium oxalate (BDH, Poole, Dorset, UK). Following excision of the lumbrical muscles they were immersed in the same oxalate-containing fixative at 4°C overnight. The tissues were then washed several times (6 × 10 min) in a solution of 7.5% sucrose, containing 90 mM potassium oxalate brought to pH 7.4 with potassium hydroxide. After washing, they were postfixed for 2 h at 4°C in a solution of 1% osmium tetroxide and 2% potassium pyroantimonate in 0.01 M acetic acid (pH 7.4, adjusted with KOH). After a 20 (2 × 10)-min rinse in distilled water brought to pH 10 with potassium hydroxide the tissues were dehydrated in an ascending ethanol series and 1,2-epoxy propane for 15 min/step and finally infiltrated with and embedded in a 1:1 mixture of Agar 100/Araldite resin.

To determine the chemical composition (calcium content) of the precipitate, mounted ultrathin (70–80 nm thick) tissue sections were immersed in a 5 mM solution (pH 7) of EGTA [ethylene glycol-bis-(β-amino ethyl ether) *N,N*-tetraacetic acid; Sigma London Chemical Co Ltd] for 2 h at 60°C. Sections were then rinsed in sterile water (20°C) and dried. Controls were incubated in sterile water under the same conditions.

Synaptic vesicle quantitation

Synaptic vesicle diameters were measured to determine whether alterations in the vesicular turnover process at the terminal may influence neuromuscular transmission during DTB intoxication. Consequently, five motor endplates were sampled from one animal on each of days 1 to 5 during treatment with DTB and compared with one control animal (day 0). One hundred synaptic vesicles lying in the vicinity of the presynaptic membrane were selected from enlarged micrographs of these terminals at a

final magnification of 50,000 – 75,000. Care was taken to ensure that whenever practicable this sample consisted of a continuous band of vesicle-filled terminal cytoplasm to reduce sampling bias. Vesicle diameter was calculated as the mean of the sum of the greatest diameter and that perpendicular to it.

The measurements derived from each endplate represented 'grouped frequency data' and were treated accordingly. Variability of synaptic vesicle diameters both within and between endplates was calculated by analysis of variance. Assessments of differences in synaptic vesicle diameters due to DTB treatment were based on comparisons of group means of five endplates per animal.

Results

Functional disturbances

The appearance and condition of the animals was similar to that described by Kemplay [25]. Control animals gained weight steadily and were alert, agile and active. Their neurological functions were normal as demonstrated by their ability to balance on and cling to a horizontal pole.

Treated animals showed no overt signs of intoxication within 1 day of the first dose of DTB, but were clearly affected following the second dose. They were withdrawn, would not grasp a horizontal pole and were reluctant to cling to and walk along it. However, they moved confidently over a flat surface, albeit less actively than normal. On the 3rd day the animals were hypothermic, showed a generalised weakness and lay quietly on the cage floor. They were just capable of lifting their heads but were incapable of drawing their limbs beneath them. Their hindlimbs appeared weaker than their forelimbs, locomotion being reduced to a slow crawl only and they were unable to grasp a horizontal pole. By day 4, the animals were incapable of movement and of consuming food and water and displayed extremely laboured breathing. Approximately half of the animals that began the experiment had died by this time; progressive respiratory failure and dehydration appeared to be contributory factors. No DTB was given to the animals after the 4th day. Animals surviving until day 5 showed these same functional disturbances.

Morphological changes in intramuscular nerves and motor endplates

The ultrastructure and function of the normal mammalian neuromuscular junction have been described extensively by Gauthier [16] and Buller [9].

Briefly, the terminal of the motor nerve (motor endplate) makes close contact with a highly specialised area of the muscle fibre sarcolemma forming the neuromuscular junction (Fig. 1). Within the motor endplate many rounded synaptic vesicles exhibiting a narrow mean size range (Table 1) are packed closely together and fill the terminal, lying subjacent to the presynaptic neurilemma. Occasionally, clusters of vesicles abut the presynaptic membrane at discrete (active) sites situated opposite the postsynaptic junctional clefts of the sarcolemma. Numerous elongate mitochondria, an occasional multivesicluar body and a few branched strands of the smooth endoplasmic reticulum (SER) are interspersed among the packed synaptic vesicles which show homogeneous (moderate) electron density. Some intermediate filaments and microtubules normally extend from the preterminal axon into the terminal forming a central core of vesicle-free axoplasm which does not impinge on the presynaptic membrane. It is noteworthy that occasionally a few, fine Schwann cell filopodial or lamellar processes, lying on the prejunctional aspect of the sarcolemmal basal lamina, partially separate the endplate from the postsynaptic junctional celfts. Preterminal axons and intramuscular myelinated fibres are unremarkable except that sometimes, small focal aggregates of the SER and/or mitochondria are found lying subjacent to the axolemma at sites of axonal varicosities (Fig. 2).

Treatment with DTB produced no ultrastructural changes in motor endplates and preterminal axons within 24 h of the first dose. However, some intramuscular myelinated nerve fibres were strikingly altered at this time with separation of the outermost myelin lamellae and hydropic Schwann cell cytoplasm which contained distended elements of the rough endoplasmic reticulum (RER) and swollen mitochondria (Fig. 3). Within the myelin sheath several large

Fig. 1. Motor endplate. Control. Terminal axoplasm is filled with elongate mitochondria and rounded synaptic vesicles which lie in close proximity to the presynaptic membrane. Some coated vesicles (*arrowheads*) and a few tubular elements of the smooth endoplasmic reticulum (SER) (*arrows*) lie between these organelles. × 34,880

Fig. 2. Intramuscular myelinated fibre. Control. Small amounts of branching tubulovesicular elements of the SER (*arrows*) associated with a few mitochondria are located at sites of axonal indentations. × 12,740

Fig. 3. Intramuscular myelinated fibre. Dithiobiuret (DTB) – day 1. Three fibres show marked hydropia of Schwann cell cytoplasm with mitochondrial swelling, while one fibre appears normal (*N*). Distended adaxonal vacuoles contain an amorphous material which resembles a serum-like fluid (*arrows*). Axoplasmic ultrastructure is unaltered apart from some increase in electron density. × 6,900

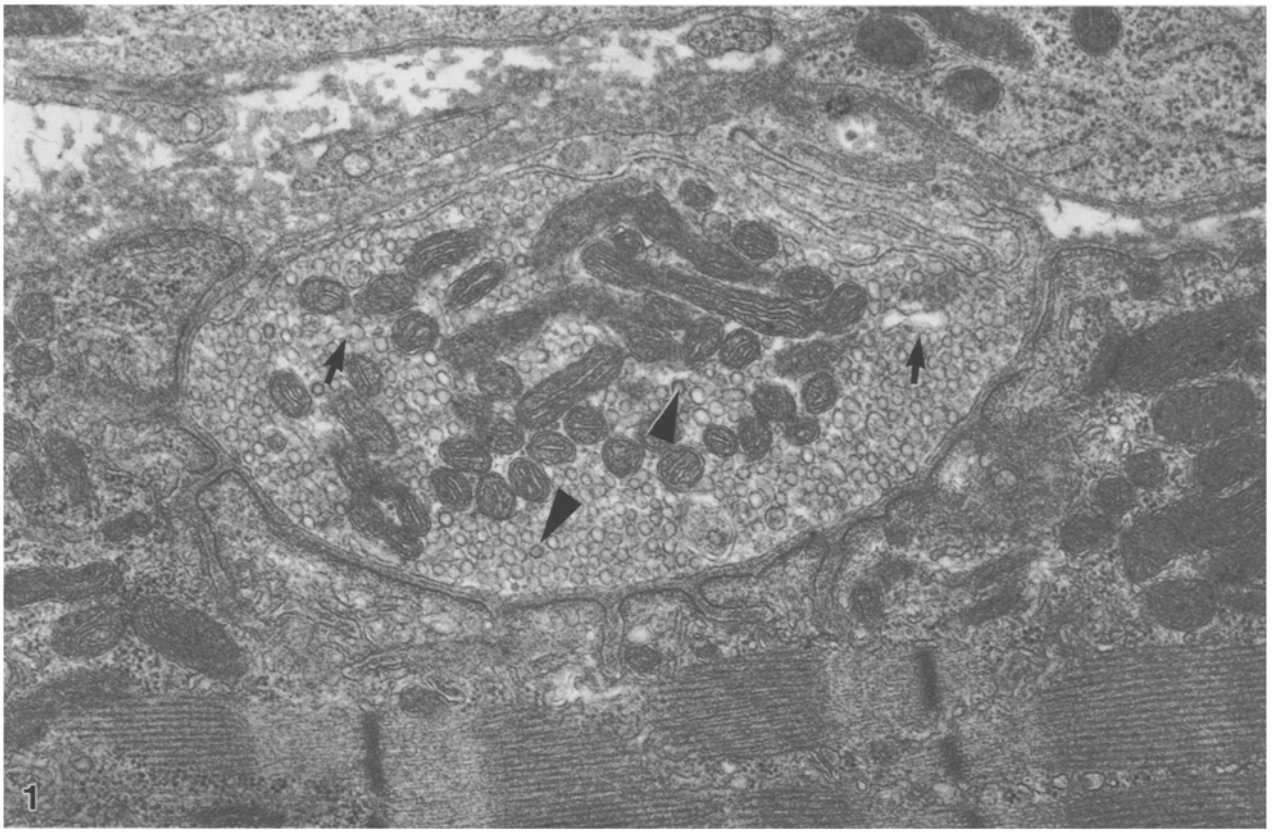

Figs. 1–3

Table 1. Synaptic vesicle quantitation

Day	Synaptic vesicle diameter $n = 100$/ endplate Mean ± 1 SD	Range (nm) $n = 100$/end plate	Group mean (nm) ± 1 SD $n = 5$ endplates	Standard error of difference of means (lower and upper limits)
0 (Control)	50.2±34.4	33.6– 67.2	49.5±33.8	–
	47.7±32.5	33.6– 67.2		
	50.5±38.3	31.1– 72.5		
	53.7±39.1	31.1– 82.8		
	45.4±25.4	30.9– 61.8		
1	53.1±68.9	32.4– 64.8	51.3±38.8	1.821 (−4.012–7.654)
	47.8±31.0	40.2– 60.3		
	51.3±36.3	33.6– 92.4		
	52.8±33.8	42.0– 67.2		
	51.5±31.3	33.6– 75.6		
2	50.3±30.1	33.6– 67.2	50.8±35.7	2.011 (−3.339–8.327)
	47.6±31.9	33.6– 67.2		
	53.6±43.2	40.2– 67.0		
	45.9±34.2	32.4– 64.8		
	56.6±41.3	40.5– 84.0		
3	47.9±33.1	33.5– 73.7	51.0±38.5	1.504 (−4.329–7.337)
	51.1±32.8	33.5– 80.4		
	50.1±36.6	33.5– 67.0		
	48.8±32.4	33.6– 67.2		
	57.2±50.0	31.1–104.0		
4	55.5±23.9	40.5– 81.0	55.4±37.1	5.898* (0.065–11.731)
	48.2±35.0	33.6– 67.2		
	57.5±38.6	42.0– 84.0		
	54.8±33.9	42.0– 67.2		
	61.1±48.6	33.6–100.8		
5	52.5±36.2	33.6– 84.0	55.5–36.3	6.019* (0.186–11.852)
	58.1±41.8	42.0–100.8		
	57.8±43.0	41.4– 93.2		
	53.9±32.8	40.2– 80.4		
	55.3±30.8	25.8– 82.4		

* Significant at 5% confidence level. $P < 0.05$

adaxonal vacuoles containing a flocculent, moderately electron-dense material were seen. Frequently, the axoplasm adjacent to these vacuoles was unusually electron dense but no other abnormal features, e.g. swollen mitochondria, were encountered. The impression that this finding was treatment-related and not of artifactual origin was strengthened by the observation that not all fibres in a small bundle were similarly affected and to the same degree.

The first change in motor endplate morphology was present on day 2. Most endplates were normal at this time but a small minority showed excessive amounts of SER arranged as membranous, interconnecting tubulovesicular profiles accumulated within the terminal and preterminal axons (Fig. 4).

By the 3rd day, some endplates retained the normal distribution of organelles, while many now showed increased numbers and packing density of synaptic

Fig. 4. Motor endplate. DTB – day 2. Masses of branching tubular SER (*arrows*) are prominent within the terminal axoplasm and represent the first indication of intoxication. ×29,500

Fig. 5. Motor endplate. DTB – day 3. Terminals congested with swollen mitochondria, synaptic vesicles, large lucent vacuoles and a few elements of tubular SER. An amorphous, moderately electron-dense material extends between these organelles (*arrow*). ×28,640

Fig. 6. Motor endplate. DTB – day 3. Similar features to Fig. 5 but note the virtual absence of synaptic vesicles from the vicinity of the presynaptic membrane indicated (*arrows*) and their replacement by some SER and amorphous material. ×27,680

Fig. 7. Motor endplate. DTB – day 3. Electron-lucent terminal axoplasm containing swollen, abnormal mitochondria and a few distended vacuoles originating from the tubular SER. ×14,360

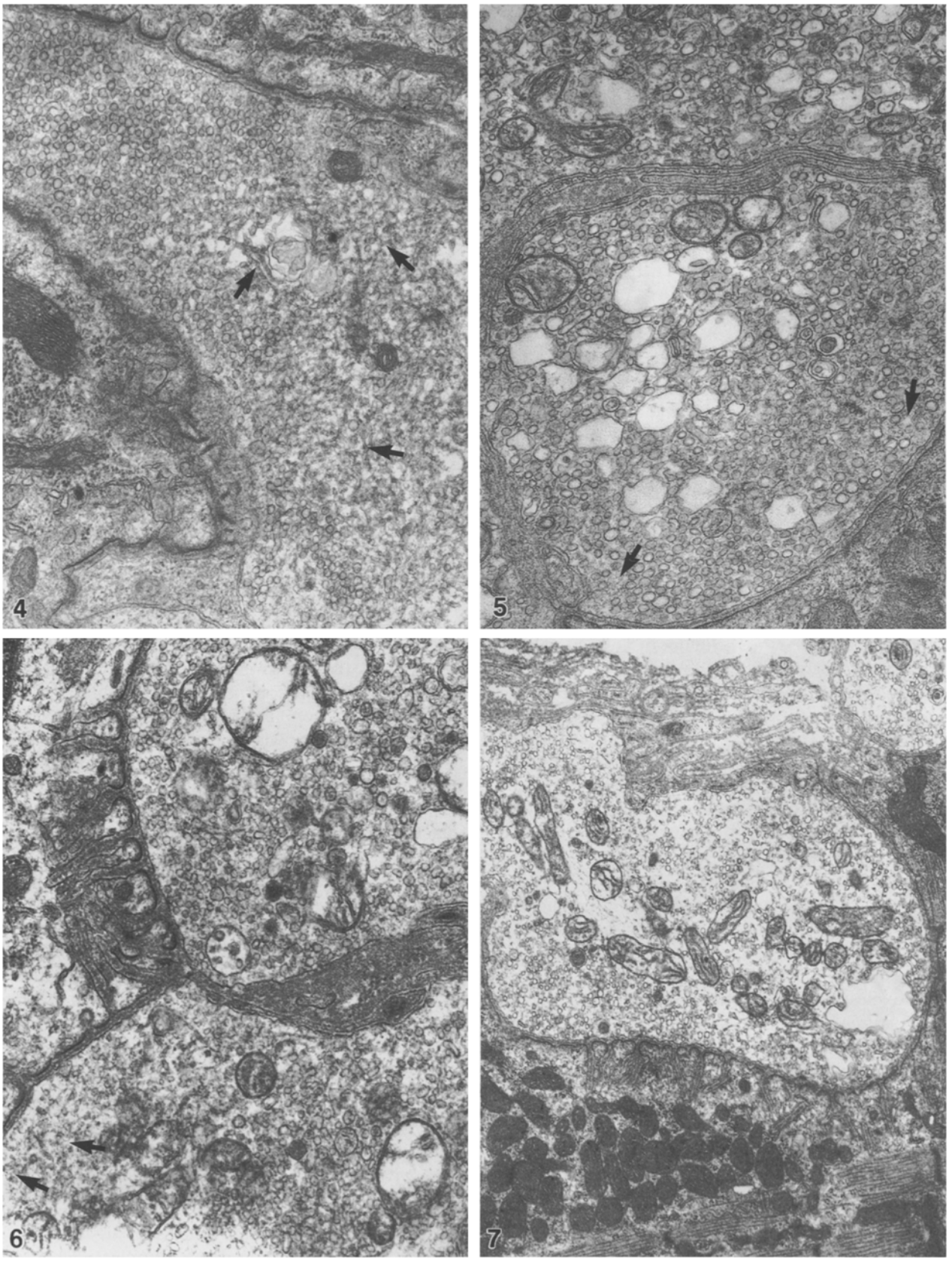

Figs. 4–7

vesicles. By comparison with controls, these latter endplates appeared more rounded and distended and contained increased numbers of dense-cored and lucent vesicles, multivesicular bodies and altered mitochondria (Fig. 5). In some, branched cisternae of the SER, myelin whorls and skeins of intermediate filaments were now more abundant. At this time too, a flocculent, amorphous material appeared in some terminals increasing their electron density (Fig. 6) and was often situated adjacent to the presynaptic membrane. In many of these, mitochondria were unusually electron lucent compared with controls and with those in adjacent Schwann cells and myocytes. Electron-lucent mitochondria were also seen in a minority of endplates which were packed with intermediate filaments, contained some membrane whorls and dilated cisternae and few synaptic vesicles (Fig. 7). No evidence of endplate degeneration or retraction was seen, although one, long unmyelinated axon originating from a myelinated fibre was encountered close to an endplate. This was regarded as being a collateral axonal sprout on the basis of dimensions and structure.

At this time, all preterminals and myelinated nerve fibres showed axoplasmic organelle segregation to a greater or lesser degree (Fig. 8) such that bundles of tangled intermediate filaments separated clusters of lucent mitochondria, microtubules or large masses of branching, tubular SER profiles. A few, membrane-bound, electron-lucent vacuoles were occasionally associated with these latter structures. Within the small groups of intramuscular myelinated fibres accumulations of tubulovesicular SER profiles were concentrated on both sides of the axonal constriction at nodes of Ranvier. Some Schwann cells investing axons with markedly altered axoplasmic structure displayed the hydropic changes described above while others appeared normal.

On day 4, many motor endplates now showed marked enlargement (Fig. 9) and distortion which was associated primarily with increased abundance and packing density of intermediate filaments and of synaptic vesicles; some of these latter were significantly larger than normal (Table 1). These were usually distributed ubiquitously throughout the terminal axoplasm, although focal clusters were sometimes seen. It is noteworthy that not all endplates showed significant alterations in synaptic vesicle diameters when compared with controls. Larger, electron-lucent vacuoles, autophagosome-like bodies, membranous whorls, dense-cored and coated vesicles were also present in greater numbers. Mitochondria were either of normal appearance or lucent and swollen as described previously. More endplates (especially those that showed marked distension) contained large amounts of branching tubular SER profiles, which usually, were associated with large bundles of intermediate filaments. Elements of the SER and individual filaments occasionally lay close to the presynaptic membrane. The amorphous material seen in some endplates on day 3 now filled more endplates and extended proximally into the preterminal axon. Interposition of Schwann cell filopodial and lamellar processes between the pre- and post-junctional membranes of the neuromuscular junction was now encountered more frequently. In some instances the extent of this interposition was such as to separate these membranes by approximately 15% – 85% of the full contact zone seen in the tissue section, thus, significantly reducing the area of functional contact between the two sides of the neuromuscular junction (Fig. 10). At this time too, some constituent parts of individual motor endplates appeared to be retracting or had retracted away from the post synaptic membrane (Fig. 11). At some neuromuscular junctions a significant proportion of endplate terminals were found to have become disassociated from the postsynaptic sarcolemmal specialisations at that junction. In some instances Schwann cell cytoplasm had replaced the presynaptic terminal at this site (Fig. 12).

In general, the changes seen in intramuscular myelinated fibres and preterminals were as described above, except that now the accumulated SER and intermediate filaments were more prominent (Fig. 13). Organelle accumulations, especially of mitochondria and SER were commonly encountered at proximal and distal paranodal axonal constrictions indicative of supply by both anterograde and retrograde axoplasmic transport, respectively. In intramuscular fibres disproportionately thin myelin sheaths were more frequently associated with axons distended with packed branching tubular SER. In one instance, an unmyelinated axon sprout was observed lying between an endplate and the last heminode of its motor axon.

On day 5 no further increase either in size of motor endplates or, in the extent of endplate retraction above that seen on the 4th day was noted. The ultrastructural features of the neuromuscular junction and intramuscular myelinated nerve fibres were similar to those described above.

No evidence of myocyte damage either at the sole plate region or elsewhere was seen at any time.

Calcium localisation

Borgers et al. [8] have suggested that the oxalate-pyroantimonate reaction in osmicated tissues produces an intensely electron-dense granular deposit at the site of Ca^{2+} location. Confirmation of the calcium

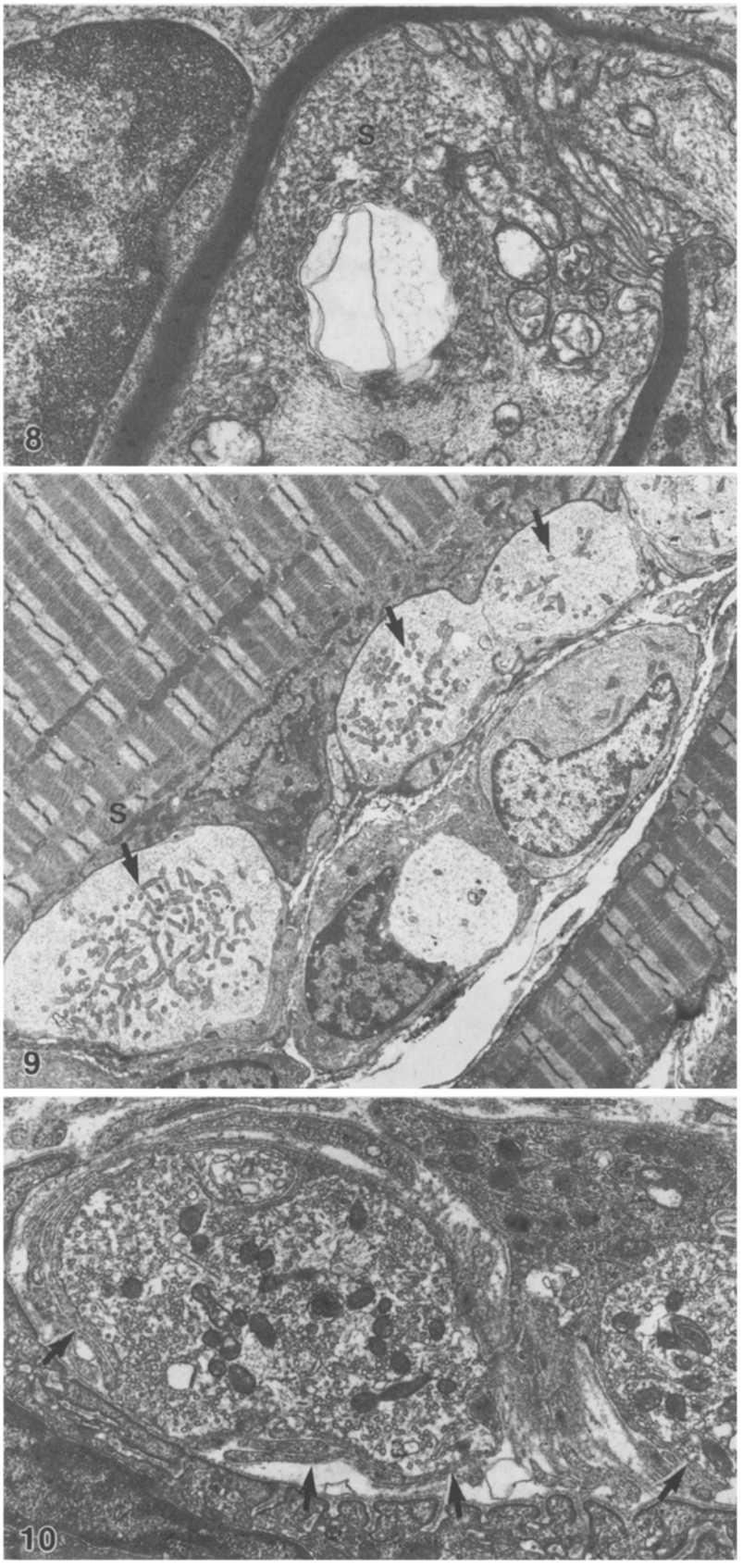

Fig. 8. Intramuscular nerve fibre – oblique section. DTB – day 3. Part of the last myelinated heminode of this fibre showing segregation of axonal organelles namely, intermediate filaments, swollen mitochondria and branching tubular SER (*S*) on the proximal side of the paranodal terminal myelin loops. ×17,420

Fig. 9. Motor endplate. DTB – day 4. Terminal swellings (*S*) and axoplasmic distension by accumulations of packed organelles. ×4,890

Fig. 10. Motor endplate. DTB – day 4. Interposition and separation of terminals from the junctional sarcolemma by Schwann cell lamellar processes (*arrows*). Note the loss of functional contact between pre- and postsynaptic membranes. ×13,360

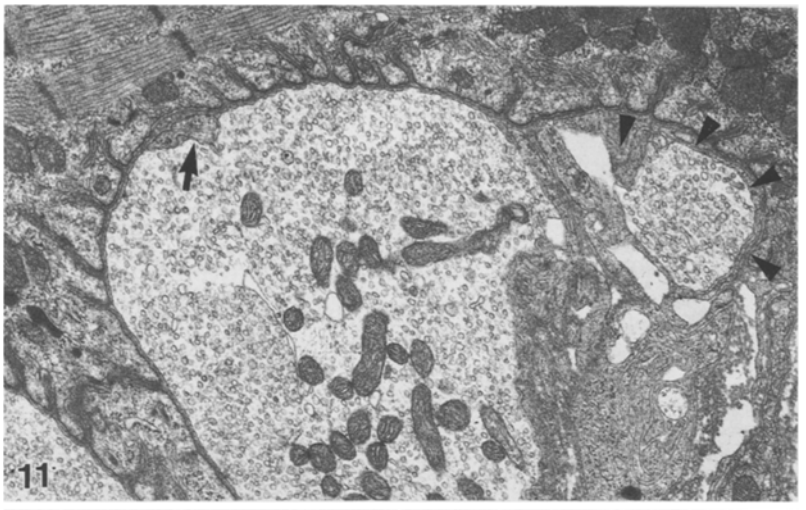

Fig. 11. Motor endplate. DTB – day 4. Interposition of Schwann cell lamellar processes between pre- and postsynaptic membranes (*arrow*). One terminal appears to be retracting away from the postsynaptic sarcolemma (*arrowheads*). ×13,900

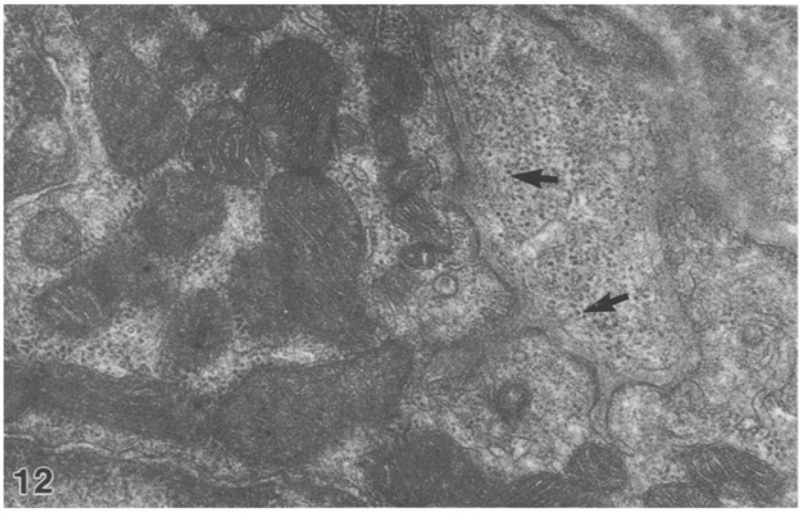

Fig. 12. Neuromuscular junction. DTB – day 5. Terminal retraction with Schwann cell cytoplasm remaining on preterminal aspect (*arrows*). ×35,620

Fig. 13. Intramuscular nerve fibre. DTB – day 5. Segregation of axoplasmic organelles into a central core (*C*) of intermediate filaments and mitochondria adjacent to peripherally displaced masses of branching tubular SER (*S*). Note the hydropic Schwann cell cytoplasm and adaxonal lucent vacuoles. ×11,750

Fig. 14a, b. Motor endplate. Control. Oxalate – pyroantimonate cytochemistry. **a** Precipitates present in almost all synaptic vesicles and in the tubular elements of the SER. Note the degree and distribution of reaction product in the sarcoplasm of the adjacent muscle fibre. **b** Increased magnification of terminal axoplasm from a motor endplate from the same animal. Precipitate is ubiquitously distributed throughout terminal organelles. The heavy deposits in mitochondria are due to artifactual swelling during fixation. **a** ×27,800; **b** ×43,500

Fig. 15 a, b. Motor endplate. DTB – day 4. **a** Degree and distribution of reaction product is reduced within these terminals showing organelle congestion while that in the adjacent sarcoplasm is similar to control levels. **b** Increased magnification of one terminal (shown in **a**) emphasising the reduction in terminal reaction product. Precipitate is reduced in both artifactually expanded mitochondria and in those abnormally swollen due to treatment. **a** ×15,360; **b** ×28,200

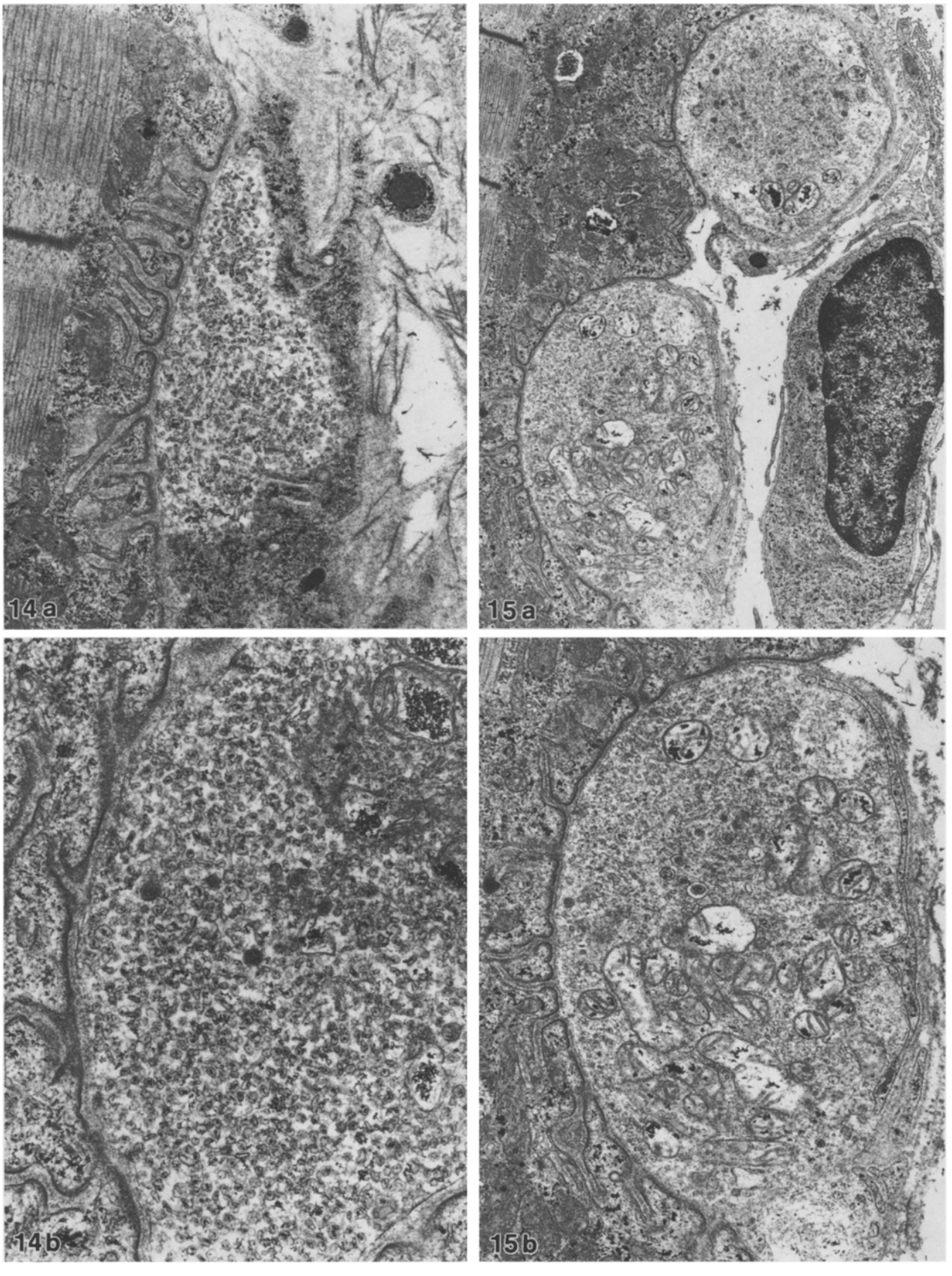

Figs. 14 and 15

content of precipitates was provided by their removal during EGTA incubation.

In morphologically normal motor endplates in functionally normal animals, electron-dense deposits were present in the majority of synaptic vesicles, the SER and multivesicular bodies (Fig. 14). Deposits were also found within these organelles in preterminals and myelinated nerve fibres. Intact mitochondria contained few, fine electron-dense particles of reaction product. However, partial mitochondrial swelling resulting as an artifact of fixation produced heavy deposition of reaction product in the expanded (disrupted) area. The sole-plate cytoplasm also contained heavy deposits with the notable exception of mitochondria which showed only a faint 'stippling' of fine granular material. Extrafibrillar sarcoplasm contained the heaviest electron-dense deposits in the vicinity of the Z-line, this being located primarily in the ground cytoplasm – very little being contained by either the sarcoplasmic reticulum or the triad system. The pattern of precipitation within the components of the sarcomere was striking. Fine granular material was frequently associated with the contractile components, especially the thick (myosin) myofilaments, often outlining the M-band with two parallel linear concentrations of particles. No deposits associated with the Z-line were seen, although the adjacent I-band often contained high densities of reaction product.

The distribution and compartmentalization of reaction product was unchanged on days 1 and 2. The tubulovesicular SER profiles seen increasingly in terminals from the 2nd day showed moderate amounts of reaction product while synaptic vesicle deposits were normal. Electron-lucent areas within the axonal and terminal SER and adaxonal vacuoles in intramuscular myelinated fibres contained heavy deposits.

In some endplates on days 3 and 4 fewer synaptic vesicles contained particulate deposits. Overall, precipitation appeared reduced (Fig. 15) by comparison with controls, especially when terminal and sole-plate cytoplasmic reaction product deposition were compared. In others, with high organelle packing density and much amorphous ground material, a sparse, fine, reaction product was present throughout the terminal cytoplasm both within and between organelles.

Discussion

Hitherto, no histological or ultrastructural evidence has been provided for pathological alterations in muscle [4], brain, spinal cord or peripheral nerves [41] of DTB-intoxicated animals. A large body of evidence derived from pharmacological and electrophysiological studies [3–5, 7, 38–41] supports the hypothesis [4, 7] that DTB neurotoxicity is manifested by an effect at the neuromuscular junction. Observations of collateral (axon) and terminal (motor endplate) sprout formation studied [25] in several muscles of DTB-intoxicated rats beginning within a few days of the initial dose lend considerable weight to the proposition that some deficit in neuromuscular transmission and not muscular performance is responsible for the functional disturbances. The importance of this observation lies in the inference that the trophic interrelationship between nerve terminal and muscle has broken down. Indeed, Ironton et al. [21] indicate that terminal sprouting arises in inactivated muscle, which during DTB intoxication appears to be produced by failure of impulse transfer at the neuromuscular junction.

The rapid onset of a functional deficit in animals treated with DTB has been demonstrated in this study to parallel closely the development of morphological changes in motor nerves and their terminals in rat lumbrical muscles. First indications of functional impairment observed between 24 and 48 h (i.e. after the second dose) are contemporaneous in some motor endplates with abundant branching tubular SER profiles. Such interconnecting SER profiles are not found in the normal preterminal and motor endplate and represent the earliest demonstrable ultrastructural change due to DTB. It is germane to this discussion to establish the morphological differences between the branching tubular SER profiles and microtubules. Microtubules are characteristically straight and unbranched and display a regular diameter of 25 ± 2 nm. By contrast, the accumulations of SER in preterminals and motor endplates comprise branching, interconnecting, membranous structures which, in places, have a diameter similar to that of microtubules but also display focal varicosities and dilatations. By the 3rd day, when severe functional impairment was evident the majority of motor endplates showed significant structural changes, a minority being unaffected. At this time, many terminals exhibited a considerable degree of 'cytoplasmic congestion' being distended with organelles not normally associated with this site and an apparent elevation in abundance, size and packing density of synaptic vesicles, 10-nm intermediate filaments, SER and mitochondria. These early indications of reduced functional efficiency are supplemented at later times (days 4 and 5) in some endplates by signs of severe functional depression, namely Schwann cell interposition at the junctional cleft, terminal retraction and sprout formation.

The first indication of intoxication, namely, the appearance of masses of tubular SER profiles in preterminal and terminal axoplasm appears to represent

the initial response to functional impairment and follows some time after the proximal lesion, possibly within a few hours of the second dose. Intoxication with zinc pyridinethione, ZPT [28–31] is characterised by SER accumulations comparable in both appearance and location to those following DTB treatment. Electron microscopic autoradiography of ligated sciatic nerves indicated that these profiles were derived from both anterograde and retrograde axoplasmic transport and led Sahenk and Mendell [32] to conclude that membrane accumulations were linked to an abnormality of 'turn around' of fast transported materials at the distal axon (terminal). However, the relationship between reduced 'turn around' and motor terminal functional deficit is not clear. Hypertrophy of tubulovesicular SER is most commonly associated with induction of hepatic microsomal drug metabolising enzymes (P-450 monooxygenases) during chronic administration of a wide variety of xenobiotic substances and has not until recently [23, 37] been correlated with drug metabolism in the nervous system. Volk et al. [34–36] have described tubulovesicular SER accumulations in cerebellar Purkinje neurons following chronic phenytoin administration to C57/BL6J mice. They suggest that SER hypertrophy develops as a consequence of neuronal cytochrome P-450 induction and that this may occur either, at the axon terminal of these neurons or, in the perikaryon followed by transport by anterograde axoplasmic flow to the terminal resulting in enlargement of the presynaptic area. Consideration of the appearance of distal axonal SER accumulations in DTB and possibly also in ZPT intoxications as a manifestation of induced drug metabolising enzymes may profit our understanding of these events.

DTB-induced defects in neuromuscular transmission and the subsequent terminal and collateral axon sprouting that result [25] are strikingly similar to the sequelae of botulinum intoxication [12, 13] and, therefore, merit consideration with regard to common bases of action. Current evidence indicates that botulinum toxin, in its several immunologically distinct forms [33], acts presynaptically to prevent acetylcholine release from cholinergic terminals. Normal function involves calcium entry into presynaptic terminals [24] followed by exocytosis of acetylcholine quanta (synaptic vesicles) at active zones [14, 18, 19]. Investigations of the involvement of disruption of Ca^{2+} dynamics in experimental botulinum intoxication are at variance with one another. Molgo and Thesleff [27] speculated that the stimulatory effect of the toxin on metabolic processes of Ca^{2+} removal from the terminal might account for blockade of transmitter release in botulinum intoxicated muscles. While the failure of calcium ionophores to restore quantal release of acetylcholine during botulinum toxin blockade led Kao et al. [22] to conclude that the toxin does not act by affecting Ca^{2+} entry into terminals and that interference with the process of exocytosis is responsible for the functional defect. Hirokawa et al. [20] in an elegant study, which made use of the observation that nerve terminal mitochondria swell and sequester Ca^{2+} following its influx into the nerve during repetitive nerve stimulation, demonstrated that botulinum toxin inhibits this influx. They reasoned that inhibition of the normal depolarization-evoked calcium fluxes, that accompanies nerve activity which provides the calcium that initiates synaptic vesicle exocytosis, is a valid basis for its mechanism of action. Antagonism of botulinum intoxication by 4-aminopyridine was explained by Metezau and Desban [26] as resulting from an increase in Ca^{2+} released from sequestered cytoplasmic stores within the nerve ending. These data are all the more intriguing when viewed with regard to the findings of Atchison et al. [7], in which 4-aminopyridine when given to DTB-intoxicated rats restored acetylcholine release during nerve-elicited muscle responses in a dose-dependent manner.

It was in the light of this evidence that calcium localisation by oxalate-pyroantimonate precipitation was undertaken in the present study of DTB intoxication to investigate whether or not some perturbation of Ca^{2+} dynamics was involved in the physiological dysfunction brought about by DTB. In control tissues, abundant calcium was present both within the terminal and the adjacent muscle fibre(s). Following DTB treatment terminal cytoplasmic precipitation was reduced – most notably in synaptic vesicles and indicative of some reduction in terminal calcium content. Differential (non-stoichiometric) calcium-oxalate/pyroantimonate reaction [10] is an improbable explanation of this result as the precipitates were extractible by EGTA and the degree and distribution of sarcoplasmic precipitation was consistent in control and DTB-treated muscle. It would appear then, that a feature of DTB intoxication involves a reduction in the terminal 'free' Ca^{2+} pool, i.e. that available for both involvement in the initiation of synaptic vesicle exocytosis and the oxalate cytochemical reaction.

We now understand that neuronal SER buffers intracellular calcium in the normal physiological range [11, 15, 17] and that this process involves ATP-dependent Ca^{2+}-transport systems similar to those which operate in the sarcoplasmic reticulum. The role of the SER in circumstances where cytosolic calcium is reduced below normal levels for relatively long periods is open to speculation. However, hypertrophy of this organelle in response to altered calcium levels may represent a reparative reaction aimed towards restoration of ionic equilibrium.

Finally, the studies of Williams et al. [40] of antagonism of DTB neurotoxicity pose new questions as to its mechanism of action and point the way for further investigations. They observed that several thiol-containing chelating agents, namely, disulfiram, diethyldithiocarbamate, D-penicillamine and cysteamine and one non-thiol-containing chelator (2,2′-dipyridyl) protected against the effects of DTB in a dose-dependent manner. Not only were the neuromuscular deficits reversed (as seen with 4-aminopyridine), but the other physiological disturbances associated with the intoxication were resolved after 5 days of treatment. In highlighting the fact that DTB and its metabolites, as well as DTB antagonists chelate divalent cations Williams et al. [40] consider several potential mechanisms of actions. First, functional impairment may result directly due to a DTB-metal chelate. Second, DTB could function as an ionophore, transporting and promoting intraneuronal accumulation of metal (possibly copper) to toxic levels. They further propose that manifestation of this toxicity may effect an uncoupling of oxidative phosphorylation, alterations in membrane structure and integrity and inhibition of fast axoplasmic transport. These hypotheses may be tested in an empirical manner by determination of motor endplate elemental composition in suitably prepared specimens by energy dispersive electron-probe X-ray microanalysis or by electron energy loss spectroscopy.

Acknowledgements. I am obliged to Professor J. B. Cavanagh, Dr. S. Kemplay and Dr. E. A. Lock for their positive comments and suggestions regarding this study and to Ms. M. McCrossan, Mrs. J. Roberts and Mr. C. Nolan for invaluable technical assistance. Mr. I. MacPherson undertook the statistical analyses.

References

1. Akert K, Sandri C (1968) An electron microscopic study of zinc iodide-osmium impregnation of neurons. I. Staining of synaptic vesicles at cholinergic junctions. Brain Res 7:286–295
2. Astwood EB, Hughes AM, Lubin M, Van der Laan WP, Adams RD (1945) Reversible paralysis of motor function in rats from the chronic administration of dithiobiuret. Science 102:196–197
3. Atchison WD, Peterson RE (1981) Potential neuromuscular toxicity of 2,4-dithiobiuret in the rat. Toxicol Appl Pharmacol 57:63–68
4. Atchison WD, Lalley PM, Cassens RG, Peterson RE (1981) Depression of neuromuscular function in the rat by chronic 2,4-dithiobiuret treatment. Neurotoxicology 2:329–346
5. Atchison WD, Yang KH, Peterson RE (1981) Dithiobiuret toxicity in the rat: evidence for latency and cumulative dose thresholds. Toxicol Appl Pharmacol 61:166–171
6. Atchison WD, Dickins J, Peterson RE (1982) Age dependence of dithiobiuret neurotoxicity in male and female rats. Neurotoxicology 3:233–242
7. Atchison WD, Mellon WS, Lalley PM, Peterson RE (1982) Dithiobiuret-induced muscle weakness in rats: evidence for a prejunctional effect. Neurotoxicology 3:44–54
8. Borgers M, de Brabander M, van Reempts J, Awouters F, Jacob WA (1977) Intranuclear microtubules in lung mast cells of guinea pigs in anaphylactic shock. Lab Invest 37:1–8
9. Buller AJ (1976) The motor endplate: function. In: Landon DN (ed) The peripheral nerve. Chapman and Hall, London, pp 495–532
10. Chandler JA (1978) The application of X-ray microanalysis in TEM to the study of ultrathin biological specimens – a review. In: Erasmus DA (ed) Electronprobe microanalysis in biology. Chapman and Hall, London, pp 37–63
11. Duce IR, Keen P (1978) Can neuronal smooth endoplasmic reticulum function as a calcium resevoir? Neuroscience 3:837–848
12. Duchen LW (1971) An electron microscopic study of the changes induced by botulinum toxin in the motor endplates of slow and fast skeletal muscle fibres of the mouse. J Neurol Sci 14:47–60
13. Duchen LW, Strich SJ (1968) The effects of botulinum toxin on the pattern of innervation of skeletal muscle in the mouse. Q J Exp Physiol 53:84–89
14. Ellisman MH, Rash JE, Staehelin LA, Porter KR (1976) Studies of excitable membranes. II. A comparison of specializations at neuromuscular junctions and nonjunctional sarcolemmas of mammalian fast and slow twitch muscle fibres. J Cell Biol 68:752–774
15. Eroglu L, Keen P (1977) Active uptake of ^{45}Ca by a microsomal fraction prepared from rat dorsal roots. J Neurochem 29:906–909
16. Gauthier GF (1976) The motor endplate: structure. In: Landon DN (ed) The peripheral nerve. Chapman and Hall, London, pp 464–488
17. Hartter DE, Burton PR, Laveri LA (1987) Distribution and calcium sequestering ability of smooth endoplasmic reticulum in olfactory axon terminals of frog brain. Neuroscience 23:371–386
18. Heuser JE, Reese TS (1972) Stimulation induced uptake and release of peroxidase from synaptic vesicles in frog neuromuscular junctions. Anat Rec 172:329–330
19. Heuser JE, Reese TS, Landis DMD (1974) Functional changes in frog neuromuscular junctions studied with freeze-fracture. J Neurocytol 3:109–131
20. Hirokawa N, Heuser JE, Evans L (1981) Structural evidence that botulinum toxin blocks neuromuscular transmission by impairing the calcium flux that normally accompanies nerve depolarisation. J Cell Biol 88:160–171
21. Ironton R, Brown MC, Holland RL (1979) Stimuli to intramuscular nerve growth. Brain Res 156:351–354
22. Kao I, Drachman DB, Price DL (1976) Botulinum toxin: mechanism of presynaptic blockade. Science 193:1256–1258
23. Kapitulnik J, Gelboin HV, Guengeric FP, Jacobowitz DM (1987) Immunohistochemical localisation of cytochrome P-450 in rat brain. Neuroscience 20:829–833
24. Katz B (1969) The release of neural transmitter substances. Liverpool University Press, Liverpool
25. Kemplay S (1984) Effects of dithiobiuret intoxication on motor endplates in sternocostalis and hindlimb muscles of female rats. Acta Neuropathol (Berl) 65:77–84
26. Metezeau P, Desban M (1982) Botulinum toxin type A: kinetics of calcium dependent paralysis of the neuromuscular junction and antagonism by drugs and animal toxins. Toxicon 20:649–654
27. Molgo J, Thesleff S (1984) Studies on the mode of action of botulinum toxin type A at the frog neuromuscular junction. Brain Res 297:309–316

28. Sahenk Z, Mendell JR (1977) Studies on the dying back process of peripheral nerves using *bis*-(N-oxo-pyridine-2-thionato) zinc II. Neurology 27:393
29. Sahenk Z, Mendell JR (1978) Abnormal retrograde axoplasmic transport in the pathogenesis of the experimental dying-back neuropathy of BOTZ. Neurology 28:357
30. Sahenk Z, Mendell JR (1979) Ultrastructural study of zinc pyridinethione-induced peripheral neuropathy. J Neuropathol Exp Neurol 38:532–550
31. Sahenk Z, Mendell JR (1979) Evidence for the distal axon as the site of axoplasmic transport abnormality in ZPT-induced neuropathy. Neurology 29:590–599
32. Sahenk Z, Mendell JR (1980) Axoplasmic transport in zinc pyridinethione neuropathy: evidence for an abnormality in distal turn around. Brain Res 186:343–353
33. Sellin LC (1981) The action of botulinum toxin at the neuromuscular junction. Med Biol 59:11–20
34. Volk B, Kirchgassner N (1985) Damage of Purkinje cell axons following chronic phenytoin administration: an animal model of distal axonopathy. Acta Neuropathol (Berl) 67:67–74
35. Volk B, Kirchgassner N, Detmar M (1986) Degeneration of granule cells following chronic phenytoin administration: an electron microscopic investigation of the mouse cerebellum. Exp Neurol 91:60–70
36. Volk B, Amelizad Z, Anagnostopoulos J, Knoth R, Oesch F (1988) First evidence of cytochrome P-450 induction in the mouse brain by phenytoin. Neurosci Lett 84:219–225
37. Walther B, Ghersi-Eggea JF, Minn A, Siest G (1986) Subcellular distribution of cytochrome P-450 in the brain. Brain Res 375:338–344
38. Weiler MH, Williams KD, Peterson RE (1986) Effects of 2,4-dithiobiuret treatment in rats on cholinergic function and metabolism of the extensor digitorum longus muscle. Toxicol Appl Pharmacol 84:220–231
39. Williams KD, Porter WR, Peterson RE (1982) Dithiobiuret metabolism in the rat. Neurotoxicology 3:221–232
40. Williams KD, Lopachin RM, Atchison WD, Peterson RE (1986) Antagonism of dithiobiuret toxicity in rats. Neurotoxicology 7:33–50
41. Williams KD, Miller MS, Boysen BG, Peterson RE (1987) Temporal analysis of dithiobiuret neurotoxicity in rats and assessment of potential non-neural causes. Toxicol Appl Pharmacol 91:212–221

Received July 27, 1988/Revised November 25, 1988/
Accepted November 28, 1988